Silylation of Deoxynucleotide Analog Yields an Orally Available Drug with Antileukemia Effects

Hiroshi Ureshino[1,2], Yuki Kurahashi[1], Tatsuro Watanabe[1], Satoshi Yamashita[3], Kazuharu Kamachi[1,2], Yuta Yamamoto[1], Yuki Fukuda-Kurahashi[1], Nao Yoshida-Sakai[1,2], Naoko Hattori[3], Yoshihiro Hayashi[4], Atsushi Kawaguchi[5], Kaoru Tohyama[6], Seiji Okada[7], Hironori Harada[4], Toshikazu Ushijima[3], and Shinya Kimura[1,2]

ABSTRACT

DNA methyltransferase inhibitors have improved the prognosis of myelodysplastic syndrome (MDS) and acute myeloid leukemia (AML). However, because these agents are easily degraded by cytidine deaminase (CDA), they must be administered intravenously or subcutaneously. Recently, two orally bioavailable DNA methyltransferase inhibitors, CC-486 and ASTX727, were approved. In previous work, we developed 5-O-trialkylsilylated decitabines that resist degradation by CDA. However, the effects of silylation of a deoxynucleotide analog and enzymatic cleavage of silylation have not been fully elucidated. Enteric administration of OR21 in a cynomolgus monkey model led to high plasma concentrations and hypomethylation, and in a mouse model, oral administration of enteric-coated OR21 led to high plasma concentrations. The drug became biologically active after release of decitabine (DAC) from OR21 following removal of the 5′-O-trisilylate substituent. Toxicities were tolerable and lower than those of DAC. Transcriptome and methylome analysis of MDS and AML cell lines revealed that OR21 increased expression of genes associated with tumor suppression, cell differentiation, and immune system processes by altering regional promoter methylation, indicating that these pathways play pivotal roles in the action of hypomethylating agents. OR21 induced cell differentiation via upregulation of the late cell differentiation drivers *CEBPE* and *GATA-1*. Thus, silylation of a deoxynucleotide analog can confer oral bioavailability without new toxicities. Both *in vivo* and *in vitro*, OR21 exerted antileukemia effects, and had a better safety profile than DAC. Together, our findings indicate that OR21 is a promising candidate drug for phase I study as an alternative to azacitidine or decitabine.

Introduction

Myelodysplastic syndrome (MDS) and acute myeloid leukemia (AML) are characterized by impaired differentiation of hematopoietic stem cells (HSCs) or hematopoietic progenitor cells (1, 2). Somatic mutations and aberrant DNA hypermethylation that silence cancer-regulating genes (e.g., tumor-suppressor genes) in these cells (3) are involved in pathogenesis and progression of MDS and AML (4–8). Epigenetic alterations lead to reduced hypermethylation, which can in turn cause reexpression of silenced tumor-regulating genes. These alterations represent novel therapeutic targets for both of these cancers (9).

Although the clinically available DNA methyltransferase (DNMT) inhibitors azacitidine (AZA) and decitabine (DAC) have improved the prognosis of MDS and AML (10, 11), they are easily degraded by cytidine deaminase (CDA), limiting their bioavailability after oral administration; consequently, they must be administered intravenously or subcutaneously. The efficacy and safety of oral AZA or DAC, as well as the combination of these drugs with CDA inhibitors, has been evaluated in clinical trials (12–14), resulting in the approval of CC-486 (oral AZA) and ASTX727 (DAC plus cedazuridine, a CDA inhibitor; refs. 13, 14).

Resistance to CDA is crucial for achieving elevated plasma concentrations of these drugs, which would in turn increase efficacy (15). Silylation of glycoproteins is known to influence their stabilities and therapeutic effects (16, 17); however, the effects of silylation of deoxynucleotide analogs and enzymatic cleavage of silylation have not been fully elucidated. In previous work, we developed 5-O-trialkylsilylated DACs that were resistant to CDA and exerted anticancer effects against solid tumors and adult T-cell leukemia/lymphoma (18, 19). In this study, we assessed the oral bioavailability and efficacy of 5-O-trialkylsilylated DAC for treatment of MDS and AML both *in vitro* and *in vivo*.

Materials and Methods

Reagents

5-O-trialkylsilylated DAC (OR2100, 2003, 2007, 2008, 2009, 2010, 2102, 2103, 2104, and 2201) was obtained from Ohara Pharmaceutical. AZA and DAC were purchased from Sigma-Aldrich. All reagents were dissolved in DMSO and stored at −20°C.

[1]Department of Drug Discovery and Biomedical Sciences, Faculty of Medicine, Saga University, Saga, Japan. [2]Division of Hematology, Respiratory Medicine and Oncology, Department of Internal Medicine, Faculty of Medicine, Saga University, Saga, Japan. [3]Division of Epigenomics, National Cancer Center Research Institute, Tokyo, Japan. [4]Laboratory of Oncology, School of Life Sciences, Tokyo University of Pharmacy and Life Sciences, Tokyo, Japan. [5]Center for Comprehensive Community Medicine, Faculty of Medicine, Saga University, Saga, Japan. [6]Department of Laboratory Medicine, Kawasaki Medical School, Kurashiki, Japan. [7]Division of Hematopoiesis, Joint Research Center for Human Retrovirus Infection, Kumamoto, Japan.

Note: Supplementary data for this article are available at Molecular Cancer Therapeutics Online (http://mct.aacrjournals.org/).

H. Ureshino and Y. Kurahashi contributed equally to this article.

Corresponding Author: Shinya Kimura, Hematology, Respiratory Medicine and Oncology, Department of Internal Medicine, Saga University School of Medicine, 5-1-1 Nabeshima, Saga 849-8501, Japan. Phone: 81-952-34-2366; Fax: 81-952-34-2017; E-mail: shkimu@cc.saga-u.ac.jp

Mol Cancer Ther 2021;20:1412–21

doi: 10.1158/1535-7163.MCT-20-1125

Pharmacokinetic studies in cynomolgus monkeys and mice

All procedures were performed at NISSEI BILIS. The study was compliant with Ohara Pharmaceutical policies on bioethics in animal work, and all procedures were compliant with the relevant national and international guidelines for the care and use of experimental animals. Procedures for pharmacokinetic studies are described in Supplementary Materials and Methods.

Cell lines and cultures

The MDS-L cell line was derived from the nonleukemic phase of a patient with MDS with refractory anemia-ringed sideroblasts (20). SKM1 cells (derived from the blast cells of a patient with MDS) were purchased from the Japanese Collection of Research Bioresources Cell Bank. HL60, THP-1, KG1a, and Kasumi-1 cell lines (derived from patients with AML) were purchased from the ATCC. AZA-resistant HL60 (HL60R) cells were established. Detailed cell culture methods are described in Supplementary Materials and Methods.

Primary patient samples

Primary samples were obtained from patients with MDS or AML. Experiments were approved by the Institutional Review Board of Saga University (Saga, Japan), and all procedures involving human participants were undertaken in accordance with the principles of the Declaration of Helsinki.

Western blot analysis

Western blot analyses were performed to assess the protein levels of DNMT1, UCK1, UCK2, and DCK. Procedures are described in Supplementary Materials and Methods.

Pyrosequencing assay of long interspersed nucleotide element-1 and the γ-globin promoter methylations

Pyrosequencing assays of long interspersed nucleotide element-1 (LINE-1) methylation were performed to assess global methylation (19). Procedures are described in Supplementary Materials and Methods. The methylation status of γ-globin promoter status was assessed in samples (peripheral blood) sequentially collected on day 0, 1, 5, 8, 12, 15, 19, 22, 26, and 29 after initiation of 5-day duodenal administration of 10.9 μmol/kg OR21, as described previously (21).

Cell proliferation

Cell proliferation was evaluated by CCK-8 assay (Dojindo) and half-maximal inhibitory concentration values (IC_{50}) were determined by nonlinear regression using the CalcuSyn software (Biosoft). Procedures for cell proliferation analyses are described in Supplementary Materials and Methods.

Flow cytometry

Antibodies used for flow cytometry are listed in Supplementary Materials and Methods. Stained samples were assessed using a FACSVerse cytometer (BD Biosciences), and data were analyzed using the FlowJo software (Tree Star).

Genome-wide DNA methylation analysis

Genome-wide DNA methylation analysis was performed using Infinium Human Methylation EPIC Bead Chips (Infinium EPIC; Illumina) as described previously (18). β-values ranged from 0 (unmethylated) to 1 (fully methylated). DNA methylation data were deposited in Gene Expression Omnibus (GEO) under accession number GSE148314.

Gene expression microarray analyses

Procedures for gene expression microarray analyses are described in Supplementary Materials and Methods. Microarray data were deposited at GEO under accession number GSE141677.

Mice

All animal experiments were approved by the Institutional Review Board of Saga University (Saga, Japan) and performed according to the University's institutional guidelines. BALB/c Rag-2/JAK3 double-deficient (BRJ) mice (22) were housed in a specific pathogen-free barrier facility; BRJ mice were used for xenograft transplantation experiments. BRJ mice received twice-weekly administration of vehicle (1% DMSO), DAC, or OR21 after xenotransplantation. Procedures for animal experiments are described in Supplementary Materials and Methods.

Statistical analysis

All statistical analyses were performed using the EZR software package (Saitama Medical Center, Jichi Medical University, Saitama, Japan; ref. 23). $P < 0.05$ was considered statistically significant.

Results

5-O-trialkylsilylated DACs have appropriate log *P* values for oral bioavailability and hypomethylating effects in the MDS cell line

In this study, we developed 5-O-trialkylsilylated DACs (Supplementary Fig. S1A). Oral absorbability is assessed according to the log *P* value, defined as the ratio of a chemical's concentrations in the octanol versus aqueous phase of a two-phase octanol/water system (24). The log *P* values of 5-O-trialkylsilylated DACs were +1.64 to +5.20; the appropriate log *P* value for oral bioavailability is +0 to +3. Determination of LINE-1 methylation levels by pyrosequencing, which measures methylation (the ratio of T to C) at each CpG position within a sequence after bisulfite treatment, yields a representative picture of global genomic DNA methylation (25, 26). Treatment with 100 nmol/L OR2100 (OR21), 2003, 2008, 2009, 2102, or 2201 significantly decreased LINE-1 methylation levels in MDS-L (Supplementary Fig. S1B). On the basis of these drug screening experiments, we defined OR21 as a promising 5-O-trialkylsilylated DAC, as in previous reports (18, 19).

Structure of OR21

OR21, a DAC prodrug, is an oligonucleotide consisting of DAC nucleoside 5′-O-trisilylate, which is protected from degradation by CDA (**Fig. 1A**). The log *P* value of OR21 is +2.14, indicating likely oral availability. The stability of the base moiety of OR21 is almost the same (half-life, 20 hours) as that of DAC in an aqueous environment (pH 6.0–7.5), and the *in vitro* stabilities of AZA and DAC are also similar (27).

Pharmacokinetics and pharmacodynamics of OR21 in cynomolgus monkeys

Initially, we investigated the pharmacokinetics of OR21 in six cynomolgus monkeys. Sequential plasma samples were taken from monkeys given the prodrug, and plasma drug concentrations were measured over time. OR21 is easily degraded by gastric acid because of its chemical structure, but direct duodenal administration of OR21 to cynomolgus monkeys resulted in absorption of the drug and subsequent release of DAC. After administration of 6.6 μmol/kg OR21, the area under the plasma drug concentration–time curve (AUC) was 0.30 (±0.18) μmol/L/hour, and after administration of 6.6 μmol/kg DAC,

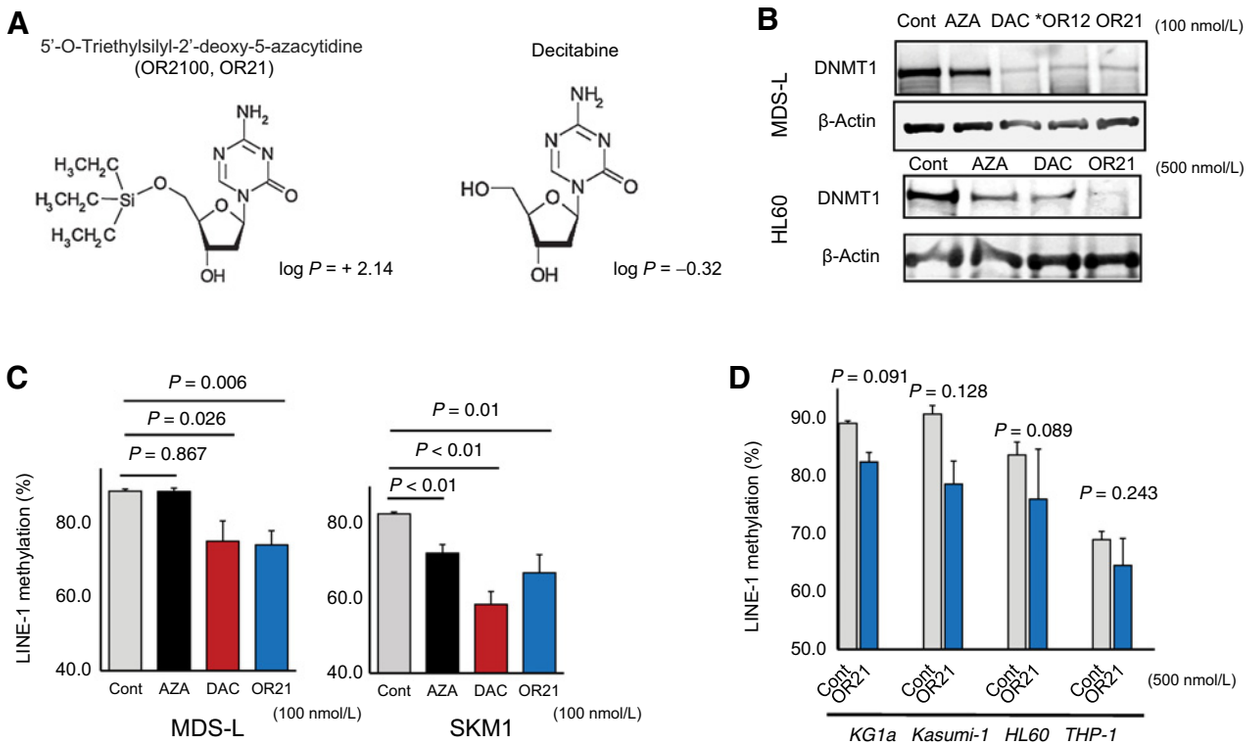

Figure 1.

Structure of OR21 and its effects on methylation. Structure of 5′-O-triethylsilyl-2′-deoxy-5-azacytidine (OR2100, OR21) and DAC (**A**). Agents with a log *P* value of +1.0 to +5.9 are expected to be absorbed after oral administration. Analysis of protein expression in MDS-L and HL60 cells treated with AZA, DAC, or OR21 (**B**). LINE-1 methylation analysis in MDS-L and SKM1 cells, as determined by bisulfite pyrosequencing (**C**). MDS-L and SKM1 cells were strongly hypermethylated (88.9% and 82.7%, respectively). Treatment with 100 nmol/L DAC or OR21 significantly decreased LINE-1 methylation levels in MDS-L [AZA, 88.8% ($P = 0.867$); DAC, 75.2% ($P < 0.01$); OR21, 74.2% ($P < 0.01$)] and SKM1 cells [AZA, 72.1% ($P < 0.01$); DAC, 58.4% ($P < 0.01$); OR21, 66.9% ($P = 0.01$)] (mean ± SD; $n = 3$). LINE-1 methylation analysis in AML cell lines treated with 500 nmol/L OR21. AML cell lines were also hypermethylated (KG1a, 89.1%; Kasumi-1, 90.7%; HL60, 83.7; THP-1, 69.0%; **D**). Treatment with OR21 tended to induce hypomethylation [KG1a, 82.4% ($P = 0.091$); Kasumi-1, 78.6% ($P = 0.128$); HL60, 76.0% ($P = 0.089$); THP-1, 64.6% ($P = 0.243$)] (mean ± SD; $n = 3$).

the AUC was 0.01 (±0.01) μmol/L/hour (**Fig. 2A** and **B**). A higher dose of DAC did not result in enteric bioavailability (Supplementary Fig. S2). Thus, OR21 exhibited higher enteric absorbability than DAC. We next evaluated the pharmacodynamics of OR21. After intravenous administration of 10.9 μmol/kg DAC, the AUC was 0.49 (±0.17) μmol/L/hour, and after duodenal administration of 10.9 μmol/kg OR21, the AUC was 0.25 (±0.14) μmol/L/hour ($n = 4$ monkeys; **Fig. 2C**). After 5-day intravenous administration of 10.9 μmol/kg DAC and duodenal administration of 10.9 μmol/kg OR21, γ-globin promoter methylation (average three CpG sites at −53, +6, +17) levels (Cont, 88.3 ± 1.35%) was significantly reduced on day 8 (DAC, 66.5 ± 2.52%, $P = 0.02$; OR21, 79.5 ± 4.50%, $P = 0.02$; **Fig. 2D**). In this setting, the demethylating effect of DAC (intravenous) was stronger than that of OR21 (duodenal administration), possibly due to differences in AUC: 9.0 mg/kg (26.3 μmol/kg) OR21 (duodenal administration) achieved an AUC of 0.45 ± 0.23 μmol/L/hour, comparable with the AUC of 1.67 mg/kg DAC (intravenous; Supplementary Fig. S2). These results indicated that OR21 has both enteral absorbability and hypomethylating effects. We next evaluated the *in vitro* and *vivo* efficacy of OR21 for AML and MDS. (At that time, the appropriately sized enteric-coated OR21 for administration *in vivo* was not available, as the enteric-coated OR21 developed for monkeys was too large to administer to mice.)

OR21 induces global DNA hypomethylation by depleting DNMT1

Hypomethylating agents (AZA and DAC) deplete DNMT1. Consistent with this, DNMT1 levels were markedly lower in two MDS (MDS-L, SKM1) and two AML (HL60, THP-1) cell lines treated with OR21 (100 or 500 nmol/L) than in untreated cells (**Fig. 1B**; Supplementary Fig. S3A–S3C). LINE-1 methylation levels were higher in both MDS-L and SKM1 cells (88.9% and 82.7%, respectively). Treatment with 100 nmol/L OR21 significantly decreased LINE-1 methylation levels in MDS-L [74.2% ($P < 0.01$)] and SKM1 [66.9% ($P = 0.01$)] cells (**Fig. 1C**); the effect was equivalent to that of 100 nmol/L DAC (75.2% reduction in MDS-L cells and 66.9% in SKM1 cells). In contrast, 100 nmol/L AZA did not decrease the LINE-1 methylation level in MDS-L; consistent with a previous report, 100 nmol/L of AZA had weak demethylating effects relative to DAC or OR21 (19). LINE-1 regions were also hypermethylated in AML cell lines (KG1a, Kasumi-1, HL60, and THP-1); in this case, 500 nmol/L OR21 tended to induce global hypomethylation (**Fig. 1D**). These results indicate that OR21 induces global genomic DNA hypomethylation in MDS and AML cell lines by depleting DNMT1, and that the effect is equivalent to that of DAC.

OR21 inhibits growth and induces apoptosis in MDS and AML cells

OR21 inhibited growth of both MDS and AML cells in a dose-dependent manner (Supplementary Fig. S4A); the effect was equivalent

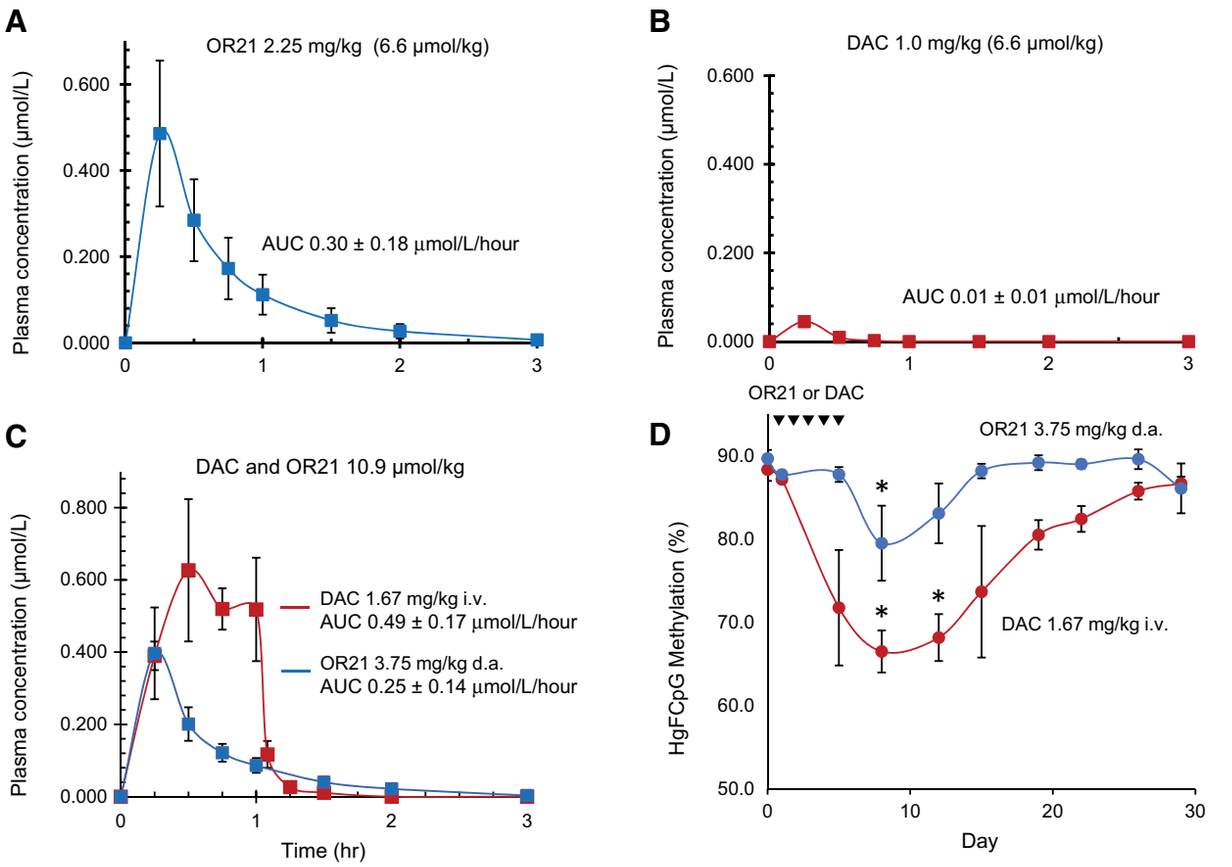

Figure 2.

Pharmacokinetics and pharmacodynamics of OR21. Sequential plasma samples were taken from monkeys given the prodrug, and plasma drug concentrations were measured over time. After administration of 6.6 µmol/kg OR21, the AUC was 0.30 (± 0.18) µmol/L/hour (**A**). After administration of 6.6 µmol/kg DAC, the AUC was 0.01 (± 0.01) µmol/L/hour (**B**). After administration of 10.9 µmol/kg DAC, the AUC was 0.49 (± 0.17) µmol/L/hour and after administration of 10.9 µmol/kg OR21, the AUC was 0.25 (± 0.14) µmol/L/hour (**C**). After 5-day intravenous administration of 10.9 µmol/kg DAC and duodenal administration (d.a.) of 10.9 µmol/kg OR21, the γ-globin promoter methylation (average three CpG sites at -53, +6, and +17) levels (Cont, 88.3 ± 1.35%) were significantly reduced at day 8 (DAC, 66.5 ± 2.52%, $P = 0.02$; OR21, 79.5 ± 4.50%, $P = 0.02$) (**D**). *, $P < 0.05$.

to that of DAC. The dose–response curves and IC_{50} values for all three agents after 72 hours of treatment are shown in Supplementary Table S1. OR21 induced apoptosis of MDS and AML cells, again in a dose-dependent manner (Supplementary Fig. S4B). In addition, OR21 induced apoptosis of primary MDS and AML cells (Supplementary Fig. S4C). These results indicate that OR21 exerts antitumor effects against MDS and AML cells.

Via regional demethylation, OR21 upregulates expression of genes associated with immune system processes, tumor suppression, and cell differentiation

Vehicle-treated HL60 and MDS-L cells shared a high proportion of hypermethylated and hypomethylated sites, and OR21-treated cells had reduced hypermethylation β-values, indicating that OR21 induced DNA demethylation (**Fig. 3A** and **B**). In the three cell lines (HL60, SKM1, and MDS-L), a heatmap comparing $\log_2$ fold changes in gene expression following OR21 treatment revealed several enriched genes, which played roles in immune system processes (e.g., *PRAME* and *CT45A*), tumor suppression (e.g., *MT1E, F, TGFβ*, and *ALOX5AP*), and cell differentiation (e.g., *EVI2A, B*, and *TYROBO*; **Fig. 3C**; Supplementary Fig. S5A–S5C). These genes were demethylated to a greater extent than others (**Fig. 3D–F**; Supplementary Fig. S6A and S6B), indicating that their expression levels were regulated by promoter DNA methylation. The demethylating effect of 500 nmol/L OR21 was similar to that of 500 nmol/L AZA (Supplementary Fig. S7A–S7C). OR21 is a prodrug of DAC; thus, the demethylating effect and gene expression profiles of OR21-treated cells were very similar to those of DAC-treated cells, as described previously (18). AZA was used as a control. MDS and AML are characterized by impaired cell differentiation of HSCs and hematopoietic progenitor cells (1); therefore, induction of cell differentiation is a potential therapeutic strategy for both forms of cancer.

OR21 induces cell differentiation via upregulation of the late cell differentiation drivers *CEBPE* and *GATA-1*

CD11b is defined as a myeloid cell differentiation marker, whereas immature cells expressed HLA-DR. Hence, we used these surface markers to assess the potential of OR21 to induce cell differentiation in MDS or AML cells. OR21 upregulated expression of CD11b and downregulated expression of HLA-DR in MDS-L cells (Supplementary Fig. S8A). SKM1 and HL60 cells also exhibited upregulation of CD11b after OR21 treatment (**Fig. 4A**; Supplementary Fig. S8B).

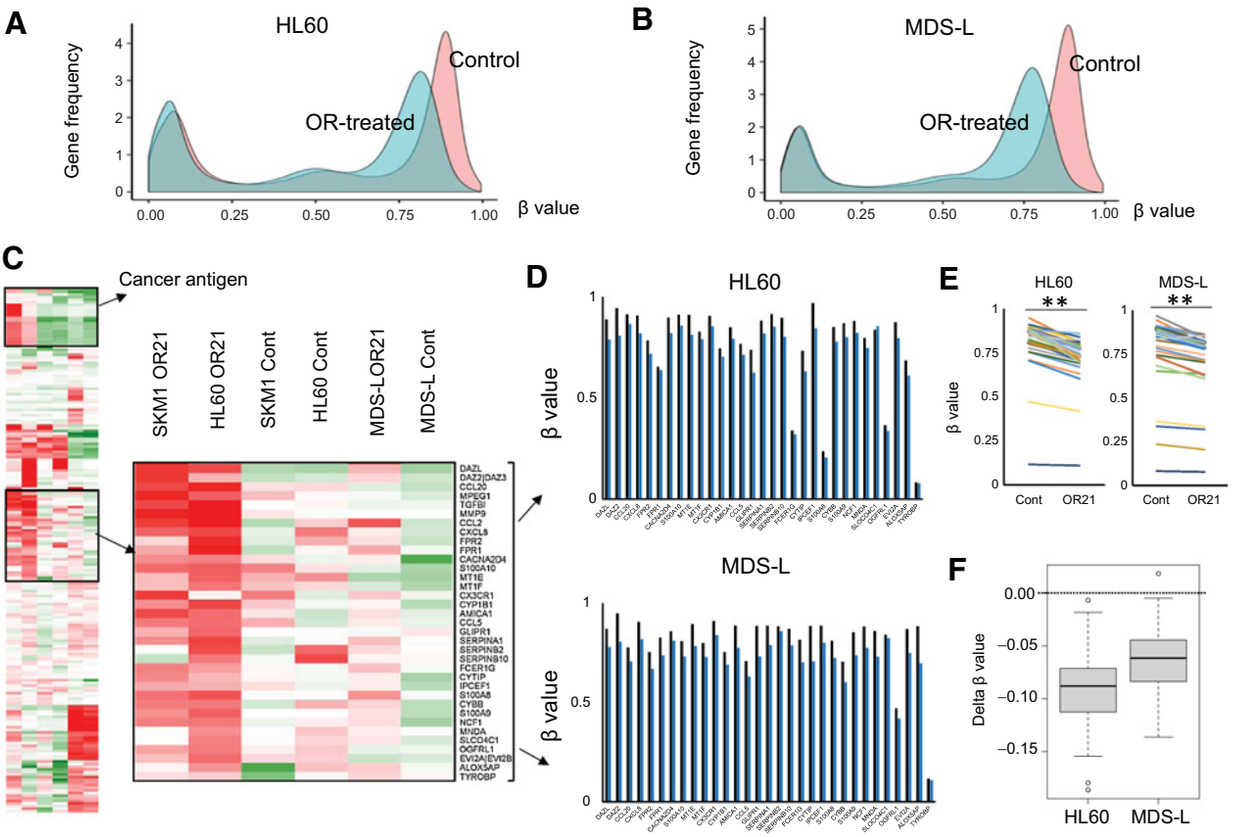

Figure 3.

Genes differentially expressed after OR21 treatment due to alteration of promoter DNA methylation. Methylome analysis revealed that OR21-treated HL60 and MDS-L cells had reduced hypermethylation β-values (**A** and **B**). Heatmap comparing $\log_2$ fold changes in gene expression among three cell lines (HL60, SKM1, and MDS-L) following treatment with OR21 (**C**). Analysis revealed enrichment of genes involved in immune system processes (including cancer testis antigen, e.g., *PRAME, TGFβ*, and *CT45A*), tumor suppression (e.g., *MT1E, F, TGFβ*, and *ALOX5AP*), and cell differentiation (e.g., *EVI2A, B, TGFβI*, and *TYROBO*). **D** and **E,** Each of these genes were demethylated after OR21 treatment (**D**). The β-values of each gene decreased (paired *t* test, **E**). **, $P < 0.01$. The delta β-values (OR21-treated minus vehicle-treated) of HL60 and MDS-L cells were below zero (**F**).

These cells also underwent morphologic changes, including a reduced nuclear–cytoplasmic ratio, larger cell size, and higher numbers of multilobed nuclei (**Fig. 4B**; Supplementary Fig. S8C), indicating that OR21 induced cell differentiation, particularly granulocytic differentiation. Hence, we used real-time quantitative reverse transcription PCR to identify the transcription factors responsible for cell differentiation. OR21 upregulated expression of the *CEBPE* and *GATA-1* mRNAs in MDS-L and SKM1 cells (**Fig. 4C**; Supplementary Fig. S8D). These results indicate that OR21 induces cell differentiation, possibly by upregulating expression of the late cell differentiation drivers *CEBPE* and *GATA-1*.

OR21 prolongs survival of MDS and AML model mice

Next, we used a mouse xenograft model to evaluate the anti-MDS efficacy of OR21. For this purpose, we intravenously injected SKM1 cells into BALB/c Rag-2/JAK3 double-deficient (BRJ) mice. Starting on day 7 posttransplantation, the mice were treated twice weekly with vehicle OR21 (**Fig. 5A**). On day 28, the number of human CD45-positive cells in peripheral blood (PB) was lower in OR21-treated mice than in vehicle-treated mice [vehicle, 6.40%; OR21, 0.31% ($P = 0.0597$); **Fig. 5B**]. In addition, OR21 prolonged survival [median overall survival; vehicle, 29 days; OR21, not reached at day 53 ($P = 0.0246$); **Fig. 5C**]. All OR21-treated mice survived with engraftment of SKM1 cells at day 53 (Supplementary Fig. S9).

Next, we used a mouse xenograft model to evaluate the anti-AML efficacy of OR21. In these experiments, BRJ mice were injected intravenously with HL60 cells and treated twice weekly with vehicle, DAC (1.0 mg/kg), or OR21(2.7 mg/kg) starting on day 5 posttransplantation (**Fig. 5D**). On day 37, the number of human CD45-positive cells in PB was significantly lower in OR21-treated mice than in vehicle-treated mice [vehicle, 2.96%; DAC, 1.67% ($P = 0.48$); OR21, 0.75% ($P = 0.049$)], and the OR21-treated mice exhibited prolonged survival [median overall survival; vehicle, 44 days; DAC, 46.5 days ($P = 0.164$); OR21, 49 days ($P = 0.005$); **Fig. 5E** and **F**]. In addition, OR21 induced significant hypomethylation of LINE-1 regions in bone marrow cells [vehicle, 83.7%; DAC, 56.3% ($P < 0.01\%$); OR21, 63.0% ($P < 0.01\%$)]. OR21-treated mice did not develop anemia, whereas DAC-treated mice were anemic at the time of sacrifice [hemoglobin levels: vehicle, 17.5 (±1.20) g/dL; DAC, 15.6 (±1.22) g/dL; OR21, 17.1(±0.31) g/dL; **Fig. 5G** and **H**]. OR21 (5.4 mg/kg) prolonged survival, whereas a high dose of DAC (2.0 mg/kg) did not [median overall survival; vehicle, 48 days; DAC, 32 days ($P = 0.040$); OR21, 57 days ($P < 0.001$); **Fig. 5I**]. Notably, DAC-treated mice died earlier than those in the other groups,

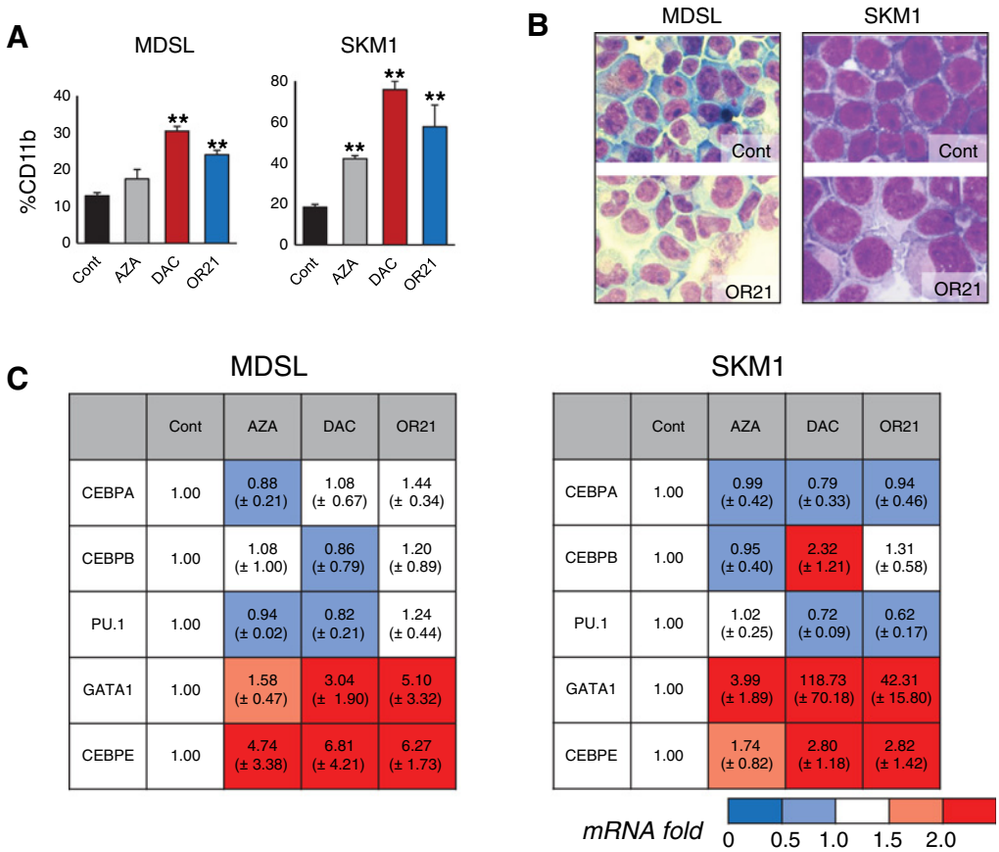

MDSL

	Cont	AZA	DAC	OR21
CEBPA	1.00	0.88 (± 0.21)	1.08 (± 0.67)	1.44 (± 0.34)
CEBPB	1.00	1.08 (± 1.00)	0.86 (± 0.79)	1.20 (± 0.89)
PU.1	1.00	0.94 (± 0.02)	0.82 (± 0.21)	1.24 (± 0.44)
GATA1	1.00	1.58 (± 0.47)	3.04 (± 1.90)	5.10 (± 3.32)
CEBPE	1.00	4.74 (± 3.38)	6.81 (± 4.21)	6.27 (± 1.73)

SKM1

	Cont	AZA	DAC	OR21
CEBPA	1.00	0.99 (± 0.42)	0.79 (± 0.33)	0.94 (± 0.46)
CEBPB	1.00	0.95 (± 0.40)	2.32 (± 1.21)	1.31 (± 0.58)
PU.1	1.00	1.02 (± 0.25)	0.72 (± 0.09)	0.62 (± 0.17)
GATA1	1.00	3.99 (± 1.89)	118.73 (± 70.18)	42.31 (± 15.80)
CEBPE	1.00	1.74 (± 0.82)	2.80 (± 1.18)	2.82 (± 1.42)

Figure 4.

OR21 induces cell differentiation in MDS and AML cells. Flow cytometry revealed elevated expression of CD11b (granulocytic differentiation marker) in MDS and SKM1 cell lines (MDS-L) following 96 hours treatment with 100 nmol/L AZA, DAC, or OR21 (mean ± SD; $n = 3$; **A**). OR21 induced morphologic changes consistent with granulocytic differentiation (i.e., reduced nuclear–cytoplasmic ratio, larger cell size, and higher numbers of multi-lobed nuclei) in MDS-L and SKM1 cells. May–Giemsa staining of cytospin preparations at 96 hours is shown. **B,** Levels of *CEBPA, CEBPB, PU.1, GATA1*, and *CEBPE* mRNAs were measured by quantitative reverse transcription PCR. Upregulation of *CEBPE* and *GATA-1* was observed in MDS-L and SKM1 cells treated with DAC or OR21 (mean ± SD; $n = 3$; **C**). *, $P < 0.05$; **, $P < 0.01$.

possibly due to severe toxicity relative to the vehicle. These results suggest that the high dose of OR21 was safer and more efficacious than a high dose of DAC. Significant cell differentiation was observed in mice exposed to late treatment (from day +28) with OR21 (vehicle, 43.3%; DAC, 75.7%, $P = 0.229$; OR21, 65.5%; $P = 0.038$; **Fig. 5J**). These results confirmed the antitumor effects of OR21 in the MDS and AML mouse models.

OR21 is effective against AZA-resistant AML cells *in vitro* and *in vivo*

Patients with MDS or AML who fail to respond to AZA treatment have limited therapeutic options, and their prognosis is extremely poor. Hence, we investigated the efficacy of OR21 against AZA-resistant AML. AZA-resistant HL60 (HL60R) cells survived in the presence of 10 μmol/L AZA. However, OR21 depleted DNMT1 protein, inhibited growth, and induced apoptosis and differentiation in these cells to a similar extent as DAC and more effectively than AZA *in vitro* (Supplementary Figs. S10A–S10C and S11). OR21 also significantly prolonged survival in the HL60R xenograft model (Supplementary Fig. S10D, $P = 0.0188$); in contrast, DAC-treated mice exhibited severe toxicity (Supplementary Fig. S12A and S12B).

Mechanism of AZA resistance

To investigate the mechanism underlying AZA resistance, we compared the protein levels of nucleoside-metabolizing enzymes between HL60 and HL60R. HL60R had lower levels of uridine-cytidine kinase 2 (UCK2; Supplementary Fig. S13A). However, *UCK2* mRNA levels and promoter methylation in proximal regions did not differ significantly between the two cell lines (Supplementary Fig. S13B and S13C). These observations suggested that depletion of UCK2 was associated with AZA resistance, but that the underlying mechanisms might not involve transcriptional regulation via altered methylation. The majority of downregulated genes in HL60R were involved in immune system processes or mitochondrial pathways (Supplementary Fig. S13D; Supplementary Table S3). HL60 methylome analysis revealed that HL60R cells were much more demethylated than HL60 (Supplementary Fig. S13E); meanwhile, the downregulated genes were less demethylated than the upregulated genes (Supplementary Fig. S13F and S13G). Pathway analysis of genes upregulated >2.0-fold revealed that genes associated with cell adhesion were upregulated in HL60R cells (Supplementary Fig. S14A and S14B). Among them, the chemokine receptor CXCR4 (Supplementary Fig. S14C and S14D) was upregulated at the mRNA and protein levels in HL60R. HL60R xenotransplant mice developed extramedullary disease

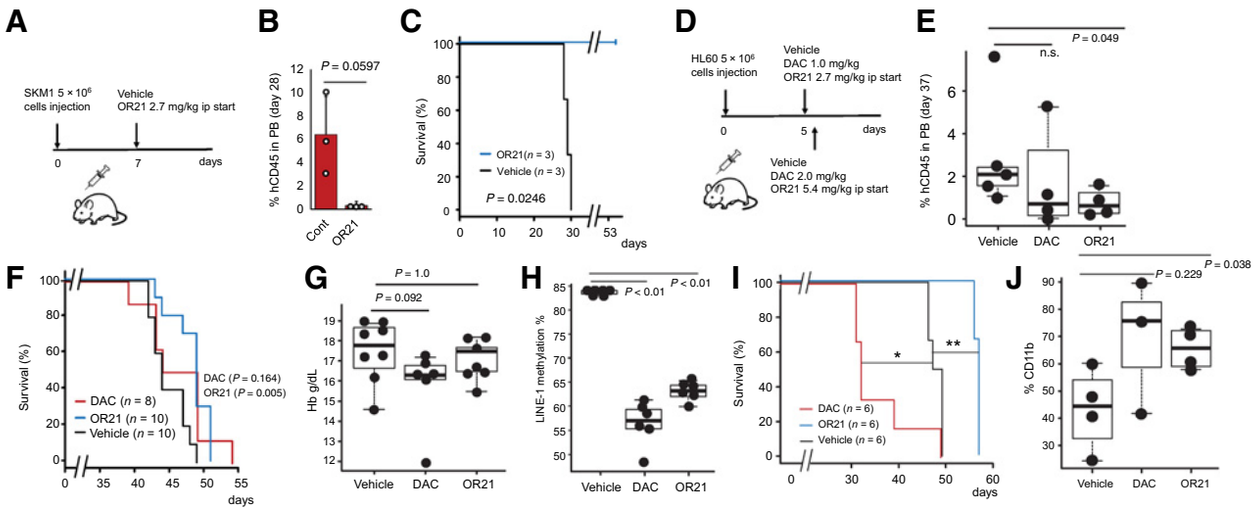

Figure 5.

SKM1 and HL60 xenograft mouse model experiments. Schedule of SKM1 cell xenograft experiments using BALB/c Rag-2/JAK3 double-deficient (BRJ) mice (**A**). Day 28: flow cytometry of hCD45-positive cells in mice treated with vehicle or OR21 (**B**). Kaplan–Meier survival curves showing cumulative survival of mice treated with vehicle or OR21 ($n = 3$ per cohort; **C**). Median overall survival time was 29 days (vehicle; $P = 0.0246$); NR = not reached. Statistical analysis was performed using the log-rank test. Schedule of HL60 cell xenograft experiments using BRJ mice (**D**). Day 37: flow cytometry of hCD45-positive cells in mice treated with vehicle ($n = 5$), DAC ($n = 4$), or OR21 ($n = 4$; **E**). Kaplan–Meier survival curves showing cumulative survival of mice treated with vehicle, DAC, or OR21 (**F**). Median overall survival times were 44 days (vehicle; $n = 10$), 46.5 days (DAC, $n = 8$, $P = 0.164$), and 49 days (OR21, $n = 10$, $P = 0.005$). Statistical analysis was performed using the log-rank test. DAC-treated mice were more likely to develop anemia than OR21-treated mice (**G**). Hemoglobin (Hb) levels were 17.5 g/dL (vehicle, $n = 8$), 15.6 g/dL (DAC, $n = 6$, $P = 0.092$), and 17.1 g/dL (OR21, $n = 7$, $P = 1.0$). LINE-1 methylation in bone marrow cells decreased after treatment with DAC or OR21 ($n = 6$ per cohort; **H**). Mice treated with a higher dose of DAC (2.0 mg/kg) did not live longer, whereas survival was prolonged in mice treated with OR21 (5.4 mg/kg) [median overall survival; vehicle, 48 days; DAC, 32 days ($P = 0.040$); OR21, 57 days ($P < 0.001$)] (**I**). HL60 xenograft mice exposed to late treatment with OR21 (day +28) had more CD11b-positive cells in PB on days +35 to +40, as determined by flow cytometry ($n = 4$ per cohort; vehicle, 43.3%; DAC, 75.7%, $P = 0.229$; OR21, 65.5%; $P = 0.038$; **J**).

(Supplementary Fig. S14E), suggesting that increases in cell adhesion activity are associated with elevated malignant potential. The changes in HL60R may be the consequence of transcriptional regulation via altered methylation.

The toxicity of OR21 may be lower than that of DAC, although both drugs have the same AUC

We monitored the long-term administration of OR21 in BALB/c mice (not immunodeficient) treated with a high (2.5 mg/kg of DAC or 7.5 mg/kg of OR21) or low (1.25 mg/kg of DAC or 3.7 mg/kg of OR21) dose of the indicated drug. Although the plasma AUCs for high-dose DAC and OR21 were approximately equal, high-dose DAC resulted in greater hematopoietic toxicity, resulting in severe anemia and early death (**Fig. 6A** and **B**). In contrast, mice treated with a high dose of OR21 developed anemia by day 29, but recovered by day 57 while still on the drug (**Fig. 6B**). In addition, these mice did not die early: all were still alive after 80 days, whereas all mice receiving high-dose DAC died within 80 days. Neither DAC- nor OR21-treated mice exhibited signs of lethal toxicity in response to low-dose DAC or OR21; however, DAC-treated mice were more likely than OR21-treated mice to develop anemia (**Fig. 6C**). Together, these results indicate that OR21 may be less toxic than DAC, resulting in improved tolerability even at high doses.

Enteric-coated OR21 exhibited favorable absorbability in an oral administration mouse model

Finally, we developed enteric-coated OR21 with the goal of making the drug resistant to gastric acid. We investigated the pharmacokinetic of enteric-coated OR21 in five ICR mice. Sequential plasma samples were taken from mice given the prodrug, and plasma drug concentrations were measured over time. Oral administration of enteric-coated OR21 to mice resulted in absorption of the drug and subsequent release of DAC. After administration of 5-mg enteric-coated OR21, the AUC of DAC (released from OR21) was 1.06 (±0.28) μmol/L/hour (Supplementary Fig. S15). Thus, enteric-coated OR21 exhibited high oral absorbability in a mouse model.

Discussion

The findings of this study reveal that OR21 is a promising hypomethylating agent that can be administered orally and exerts antitumor effects against MDS and AML both *in vitro* and *in vivo*. In addition, OR21 is less toxic than DAC. DAC and OR21 had similar effects *in vitro* in terms of hypomethylation, cell growth inhibition, and apoptosis induction; these effects were distinct from those of AZA. These differences are consistent with previous results showing that AZA is incorporated predominantly into RNA, whereas DAC is incorporated predominantly into DNA (27). Hence, the *in vitro* activity of OR21, which was triggered by release of DAC from OR21 after removal of the 5′-O-trisilylate substituent, might be due to incorporation of DNA rather than RNA.

Resistance to CDA is crucial for achieving elevated plasma concentrations of DNMT inhibitors. Guadecitabine, which is resistant to CDA and exerts stronger hypomethylating activity than AZA (28), has a favorable survival outcome in patients with MDS and AML who are not responsive to AZA (15). Nevertheless, guadecitabine is not orally absorbable (29). In contrast, the recently approved agents CC-486 (13) and ASTX727 (14) can be orally absorbed. Silylation of DAC confers resistance to CDA (18); accordingly, OR21 was enterically bioavailable in a cynomolgus monkey model, and enteric-coated OR21

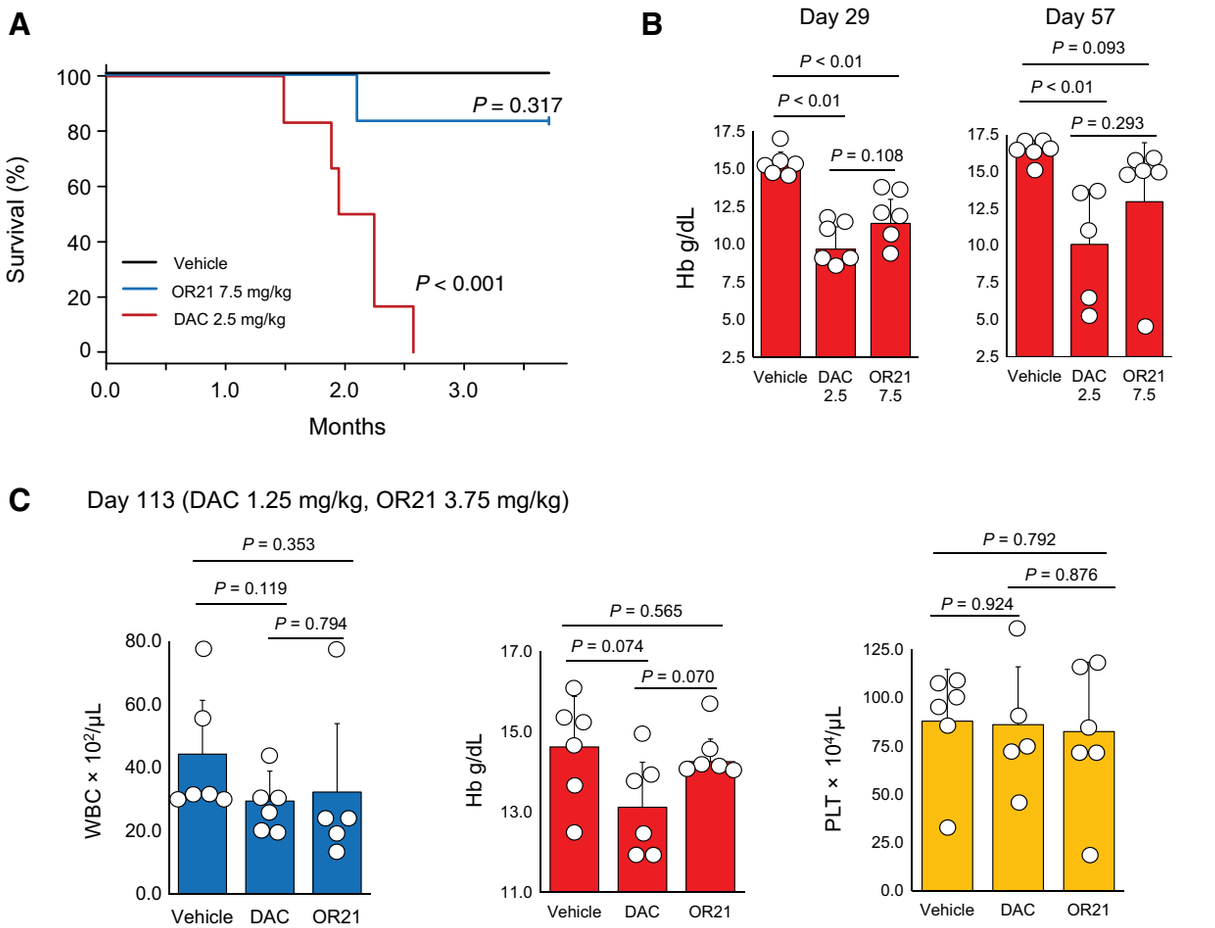

Figure 6.

In vivo safety profile of OR21. **A,** Kaplan–Meier survival curves showing cumulative survival of mice treated with vehicle, decitabine (DAC; 2.5 mg/kg), or OR21 (7.5 mg/kg; $n = 6$ per cohort). **B,** DAC (2.5 mg/kg) exerted high levels of toxicity, causing severe anemia by days +29 and +57. Mice treated with OR21 (7.5 mg/kg) also developed anemia by day +29, but recovered by day +57 while still on the drug ($n = 6$ per cohort). **C,** Among mice exposed to low-dose DAC (1.25 mg/kg) or OR21 (3.75 mg/kg) until day +113, those exposed to DAC were more likely to develop anemia ($n = 6$ per cohort). WBC, white blood cell count; Hb, hemoglobin; platelet count, PLT.

was orally bioavailable in a mouse mice model. In addition, silylation of DAC and enzymatic cleavage of silylation did not result in new toxicities *in vivo*. It is worth noting that ASTEX727 consists of two compounds, DAC and cedazuridine, a CDA inhibitor, whereas OR21 is a single compound (DAC prodrug). Consequently, OR21 has enormous advantages in terms of production, that is, it is easier and cheaper to manufacture. We have now prepared gelatin capsules filled with granules of enteric-coated OR21, and we are currently performing pharmacokinetic studies of this formulation in cynomolgus monkeys to determine the dose for a first-in-human clinical trial. Because formulation is a very important issue related to future development, we prefer not to present detailed pharmacokinetic data until the first in-human clinical trial is completed. The preliminary results suggest that OR21 could be used as an oral hypomethylating agent.

OR21-induced global DNA hypomethylation in MDS and AML cells could upregulate expression of silenced genes associated with tumor suppression, cell differentiation, and immune system processes. Among the genes that were upregulated after OR21 treatment, TGFβ is an important tumor-suppressor gene in hematologic malignancies that affects immune system process and cell differentiation (30); accordingly, TGFβ may play an important role in the antitumor effects of OR21. Although it is unclear how immune system process pathways are involved in the antitumor effects of OR21, these pathways were downregulated in AZA-resistant HL60 cells (31), suggesting that immune pathways play important roles in the antitumor effects of hypomethylating agents used to treat AML. Moreover, upregulation of genes associated with immune system processes and tumor suppression could alter immunogenicity or tumor recognition, thereby sensitizing various tumors (32, 33). Immune checkpoint inhibitors used to treat melanoma (34), lung cancer (35), or other solid tumors (36, 37) also exhibit antitumor effects in patients with MDS or AML (38, 39). To optimize promising combination therapeutic strategies involving OR21, subsequent administration of immune checkpoint inhibitors may improve efficacy against MDS or AML.

AZA-resistant HL60R cells exhibited downregulation of the UCK2 protein without alteration of *UCK2* promoter methylation or mRNA levels (40, 41). UCK2 is a pivotal uridine-metabolizing enzyme (42). Furthermore, alteration of promoter methylation resulted in

upregulation of genes related to cell adhesion in AZA-resistant HL60R cells, and OR21 overcame AZA resistance. Patients with MDS or AML who fail to respond to AZA treatment have limited therapeutic options, and their prognosis is extremely poor (43, 44). We showed that OR21 was effective agaist AZA-resistant AML *in vitro* and *in vivo*, whereas DAC exerted a high degree of toxicity *in vivo*. These results suggest that OR21 may yield clinically favorable outcomes in patients with MDS or AML who do not respond to AZA.

Patients with MDS or AML exhibit altered HSC differentiation (1, 2), and patients who have AML with low *CEBPE* gene expression level had significantly worse survival outcomes (Supplementary Fig. S16); therefore, induction of appropriate cell differentiation is a potential therapeutic strategy for MDS and AML (45, 46). In three different cell lines, OR21 upregulated genes associated with cell differentiation, resulting in induction of myeloid cell differentiation. Induction of global DNA hypomethylation triggered upregulation of the silenced key differentiation drivers *CEBPE* and *GATA-1*, which are inactivated in MDS and AML (47, 48), thereby triggering cell differentiation (49). OR21 induced antitumor effects *in vivo* by promoting both hypomethylation and cell differentiation. The effects were similar to those of DAC, although OR21 did not induce severe toxicities in mice. Long-term administration experiments confirmed that OR21 was less toxic than DAC at both high and low doses. Although it is not clear why the toxicity of OR21 is lower than that of DAC, one possible explanation is that OR21 achieves a lower peak plasma concentration: the peak plasma concentration of DAC in mice was 0.43 μmol/L after intraperitoneal administration of 1.59 μmol/L/kg OR21, versus 0.64 μmol/L after administration of 0.88 μmol/L/kg DAC (calculated as an AUC equivalent to that of released DAC, which had an AUC of 0.38 μmol/L/hour; Supplementary Table S4; ref. 18).

Although the safety of cleaved sialylated DAC has not been fully elucidated, we confirmed that OR21 is less toxic, possibly due to differences in peak plasma concentration and AUC profiles relative to DAC administration. Meanwhile, the efficacy of OR21 is mainly due to the release of DAC from OR21 after removal of the 5′-O-trisilylate substituent. Therefore, OR21 represents an orally bioavailable drug with antitumor effects against MDS and AML similar to those of DAC, and is therefore a potentially suitable treatment for patients with MDS and AML (10, 50).

In conclusion, silylation of deoxynucleotide analog can provide oral bioavailability without new toxicities. OR21 exhibits high oral availability and exerts strong antitumor effects against MDS and AML both *in vitro* and *in vivo*; moreover, it is less toxic than DAC. We anticipate that the efficacy and safety of OR21 for treatment of MDS and AML will be verified in planned early-phase clinical trials.

Authors' Disclosures

H. Ureshino reports grants from Ohara Pharmaceutical Co., Ltd. during the conduct of the study; in addition, H. Ureshino has a patent for OR2100 issued. Y. Kurahashi reports personal fees from Ohara Pharmaceutical Co., Ltd. during the conduct of the study; in addition, Y. Kurahashi has a patent with Ohara Pharmaceutical Co., Ltd. issued. T. Watanabe reports grants from Ohara Pharmaceutical Co., Ltd. during the conduct of the study; in addition, T. Watanabe has a patent for Ohara Pharmaceutical Co., Ltd. issued. K. Kamachi reports grants from Ohara Pharmaceutical Co., Ltd. during the conduct of the study; grants from Ohara Pharmaceutical Co., Ltd. outside the submitted work; in addition, K. Kamachi has a patent for OR-2100 issued. Y. Yamamoto reports grants from Ohara Pharmaceutical Co., Ltd. during the conduct of the study; grants from Ohara Pharmaceutical Co., Ltd. outside the submitted work; in addition, Y. Yamamoto has a patent for OR-2100 issued. Y. Fukuda-Kurahashi reports personal fees from Ohara Pharmaceutical Co., Ltd. during the conduct of the study; in addition, Y. Fukuda-Kurahashi has a patent for Ohara Pharmaceutical Co., Ltd. issued. N. Yoshida-Sakai reports a patent for OR2100 issued. N. Hattori reports grants from Ohara Pharmaceutical Co., Ltd. during the conduct of the study; in addition, N. Hattori has a patent for OR-21 structure issued. T. Ushijima reports grants from AMED and Ohara Pharmaceutical Co., Ltd. during the conduct of the study; grants from AMED, grants from JSPS, and nonfinancial support from Sysmex outside the submitted work; in addition, T. Ushijima has a patent for OR21 structure issued. S. Kimura reports grants from Ohara Pharmaceutical Co., Ltd. during the conduct of the study; personal fees from Bristol Myers Squibb, Otsuka Pharmaceutical, Pfizer, Novartis; grants from Chugai Pharmaceutical, Kyowa Kirin, Nippon Shinyaku, Taiho Pharmaceutical, Ono Pharmaceutical, Takeda Pharmaceutical, CSL Behring, Otsuka, and Daiichi Sankyo outside the submitted work; in addition, S. Kimura has a patent. No disclosures were reported by the other authors.

Authors' Contributions

H. Ureshino: Resources, data curation, formal analysis, validation, investigation, visualization, writing–original draft, writing–review and editing. **Y. Kurahashi:** Data curation, formal analysis, visualization. **T. Watanabe:** Data curation, supervision, visualization, writing–review and editing. **S. Yamashita:** Data curation, formal analysis. **K. Kamachi:** Data curation, writing–review and editing. **Y. Yamamoto:** Data curation. **Y. Fukuda-Kurahashi:** Data curation. **N. Yoshida-Sakai:** Data curation. **N. Hattori:** Data curation, supervision. **Y. Hayashi:** Supervision. **A. Kawaguchi:** Formal analysis. **K. Tohyama:** Resources, supervision. **S. Okada:** Resources, supervision. **H. Harada:** Resources, supervision. **T. Ushijima:** Supervision. **S. Kimura:** Conceptualization, supervision, funding acquisition, writing–review and editing.

Acknowledgments

This work was supported by Ohara Pharmaceutical Co., Ltd.

The costs of publication of this article were defrayed in part by the payment of page charges. This article must therefore be hereby marked *advertisement* in accordance with 18 U.S.C. Section 1734 solely to indicate this fact.

Received December 28, 2020; revised March 15, 2021; accepted May 25, 2021; published first May 27, 2021.

References

1. Tefferi A, Vardiman JW. Myelodysplastic syndromes. N Engl J Med 2009;361:1872–85.
2. Jordan CT. Unique molecular and cellular features of acute myelogenous leukemia stem cells. Leukemia 2002;16:559–62.
3. Jiang Y, Dunbar A, Gondek LP, Mohan S, Rataul M, O'Keefe C, et al. Aberrant DNA methylation is a dominant mechanism in MDS progression to AML. Blood 2009;113:1315–25.
4. Esteller M. Relevance of DNA methylation in the management of cancer. Lancet Oncol 2003;4:351–8.
5. Lugthart S, Figueroa ME, Bindels E, Skrabanek L, Valk PJM, Li Y, et al. Aberrant DNA hypermethylation signature in acute myeloid leukemia directed by EVI1. Blood 2011;117:234–41.
6. Cancer Genome Atlas Research Network; Ley TJ, Miller C, Ding L, Raphael BJ, Mungall AJ, et al. Genomic and epigenomic landscapes of adult *de novo* acute myeloid leukemia. N Engl J Med 2013;368:2059–74.
7. Garg M, Nagata Y, Kanojia D, Mayakonda A, Yoshida K, Haridas Keloth S, et al. Profiling of somatic mutations in acute myeloid leukemia with FLT3-ITD at diagnosis and relapse. Blood 2015;126:2491–501.
8. Kirtonia A, Pandya G, Sethi G, Pandey AK, Das BC, Garg M. A comprehensive review of genetic alterations and molecular targeted therapies for the implementation of personalized medicine in acute myeloid leukemia. J Mol Med 2020;98:1069–91.
9. Potapova A, Hasemeier B, Römermann D, Metzig K, Göhring G, Schlegelberger B, et al. Epigenetic inactivation of tumour suppressor gene KLF11 in myelodysplastic syndromes. Eur J Haematol 2010;84:298–303.

10. Fenaux P, Mufti GJ, Hellstrom-Lindberg E, Santini V, Finelli C, Giagounidis A, et al. Efficacy of azacitidine compared with that of conventional care regimens in the treatment of higher-risk myelodysplastic syndromes: a randomised, open-label, phase III study. Lancet Oncol 2009;10:223–32.
11. Jabbour E, Short NJ, Montalban-Bravo G, Huang X, Bueso-Ramos C, Qiao W, et al. Randomized phase 2 study of low-dose decitabine vs low-dose azacitidine in lower-risk MDS and MDS/MPN. Blood 2017;130:1514–22.
12. Lavelle D, Vaitkus K, Ling Y, Ruiz MA, Mahfouz R, Ng KP, et al. Effects of tetrahydrouridine on pharmacokinetics and pharmacodynamics of oral decitabine. Blood 2012;119:1240–7.
13. Savona MR, Kolibaba K, Conkling P, Kingsley EC, Becerra C, Morris JC, et al. Extended dosing with CC-486 (oral azacitidine) in patients with myeloid malignancies. Am J Hematol 2018;93:1199–206.
14. Savona MR, Odenike O, Amrein PC, Steensma DP, DeZern AE, Michaelis LC, et al. An oral fixed-dose combination of decitabine and cedazuridine in myelodysplastic syndromes: a multicentre, open-label, dose-escalation, phase 1 study. Lancet Haematol 2019;6:e194–203.
15. Sébert M, Renneville A, Bally C, Peterlin P, Beyne-Rauzy O, Legros L, et al. A phase II study of guadecitabine in higher-risk myelodysplastic syndrome and low blast count acute myeloid leukemia after azacitidine failure. Haematologica 2019; 104:1565–71.
16. Kwak C-Y, Park S-Y, Lee C-G, Okino N, Ito M, Kim JH. Enhancing the sialylation of recombinant EPO produced in CHO cells via the inhibition of glycosphingolipid biosynthesis. Sci Rep 2017;7:13059.
17. Ghafarinazari A, Paterlini V, Cortelletti P, Bettotti P, Scarpa M, Daldosso N. Optical study of diamine coupling on carboxyl-functionalized mesoporous silicon. J Nanosci Nanotechnol 2017;17:1240–246.
18. Hattori N, Sako M, Kimura K, Iida N, Takeshima H, Nakata Y, et al. Novel prodrugs of decitabine with greater metabolic stability and less toxicity. Clin Epigenetics 2019;11:111.
19. Watanabe T, Yamashita S, Ureshino H, Kamachi K, Kurahashi Y, Fukuda-Kurahashi Y, et al. Targeting aberrant DNA hypermethylation as a driver of ATL leukemogenesis by using the new oral demethylating agent OR-2100. Blood 2020;136:871–84.
20. Tsujioka T, Yokoi A, Itano Y, Takahashi K, Ouchida M, Okamoto S, et al. Five-aza-2′-deoxycytidine-induced hypomethylation of cholesterol 25-hydroxylase gene is responsible for cell death of myelodysplasia/leukemia cells. Sci Rep 2015; 5:16709.
21. Lavelle D, Saunthararajah Y, Vaitkus K, Singh M, Banzon V, Phiasivongsva P, et al. S110, a novel decitabine dinucleotide, increases fetal hemoglobin levels in baboons (P. anubis). J Transl Med 2010;8:92.
22. Ono A, Hattori S, Kariya R, Iwanaga S, Taura M, Harada H, et al. Comparative study of human hematopoietic cell engraftment into Balb/c and C57BL/6 strain of rag-2/Jak3 double-deficient mice. J Biomed Biotechnol 2011;2011:539748.
23. Kanda Y. Investigation of the freely available easy-to-use software "EZR" for medical statistics. Bone Marrow Transplant 2013;48:452–8.
24. Franklin SJ, Younis US, Myrdal PB. Estimating the aqueous solubility of pharmaceutical hydrates. J Pharm Sci 2016;105:1914–9.
25. Kazazian HH. Mobile elements: drivers of genome evolution. Science 2004;303: 1626–32.
26. Yang AS. A simple method for estimating global DNA methylation using bisulfite PCR of repetitive DNA elements. Nucleic Acids Res 2004;32:e38.
27. Hollenbach PW, Nguyen AN, Brady H, Williams M, Ning Y, Richard N, et al. A comparison of azacitidine and decitabine activities in acute myeloid leukemia cell lines. PLoS One 2010;5:e9001.
28. Fazio C, Covre A, Cutaia O, Lofiego MF, Tunici P, Chiarucci C, et al. Immunomodulatory properties of DNA hypomethylating agents: selecting the optimal epigenetic partner for cancer immunotherapy. Front Pharmacol 2018;9:1443.
29. Kantarjian HM, Roboz GJ, Kropf PL, Yee KWL, O'Connell CL, Tibes R, et al. Guadecitabine (SGI-110) in treatment-naive patients with acute myeloid leukaemia: phase 2 results from a multicentre, randomised, phase 1/2 trial. Lancet Oncol 2017;18:1317–26.
30. Dong M, Blobe GC. Role of transforming growth factor-beta in hematologic malignancies. Blood 2006;107:4589–96.
31. Leung KK, Nguyen A, Shi T, Tang L, Ni X, Escoubet L, et al. Multiomics of azacitidine-treated AML cells reveals variable and convergent targets that remodel the cell-surface proteome. Proc Natl Acad Sci U S A 2019;116:695–700.
32. Krishnadas DK, Bai F, Lucas KG. Cancer testis antigen and immunotherapy. ImmunoTargets Ther 2013;2:11–9.
33. Morris LGT, Chan TA. Therapeutic targeting of tumor suppressor genes. Cancer 2015;121:1357–68.
34. Wolchok JD, Chiarion-Sileni V, Gonzalez R, Rutkowski P, Grob J-J, Cowey CL, et al. Overall survival with combined nivolumab and ipilimumab in advanced melanoma. N Engl J Med 2017;377:1345–56.
35. Borghaei H, Paz-Ares L, Horn L, Spigel DR, Steins M, Ready NE, et al. Nivolumab versus docetaxel in advanced nonsquamous non-small-cell lung cancer. N Engl J Med 2015;373:1627–39.
36. Sharma P, Retz M, Siefker-Radtke A, Baron A, Necchi A, Bedke J, et al. Nivolumab in metastatic urothelial carcinoma after platinum therapy (CheckMate 275): a multicentre, single-arm, phase 2 trial. Lancet Oncol 2017;18:312–22.
37. Overman MJ, McDermott R, Leach JL, Lonardi S, Lenz H-J, Morse MA, et al. Nivolumab in patients with metastatic DNA mismatch repair-deficient or microsatellite instability-high colorectal cancer (CheckMate 142): an open-label, multicentre, phase 2 study. Lancet Oncol 2017;18:1182–91.
38. Daver N, Boddu P, Garcia-Manero G, Yadav SS, Sharma P, Allison J, et al. Hypomethylating agents in combination with immune checkpoint inhibitors in acute myeloid leukemia and myelodysplastic syndromes. Leukemia 2018;32: 1094–105.
39. Ravandi F, Assi R, Daver N, Benton CB, Kadia T, Thompson PA, et al. Idarubicin, cytarabine, and nivolumab in patients with newly diagnosed acute myeloid leukaemia or high-risk myelodysplastic syndrome: a single-arm, phase 2 study. Lancet Haematol 2019;6:e480–8.
40. Valencia A, Masala E, Rossi A, Martino A, Sanna A, Buchi F, et al. Expression of nucleoside-metabolizing enzymes in myelodysplastic syndromes and modulation of response to azacitidine. Leukemia 2014;28:621–8.
41. Sripayap P, Nagai T, Uesawa M, Kobayashi H, Tsukahara T, Ohmine K, et al. Mechanisms of resistance to azacitidine in human leukemia cell lines. Exp Hematol 2014;42:294–306.
42. Tomoike F, Nakagawa N, Fukui K, Yano T, Kuramitsu S, Masui R. Indispensable residue for uridine binding in the uridine-cytidine kinase family. Biochem Biophys Reports 2017;11:93–98.
43. Duong VH, Lin K, Reljic T, Kumar A, Al Ali NH, Lancet JE, et al. Poor outcome of patients with myelodysplastic syndrome after azacitidine treatment failure. Clin Lymphoma Myeloma Leuk 2013;13:711–5.
44. Prébet T, Gore SD, Thépot S, Esterni B, Quesnel B, Beyne Rauzy O, et al. Outcome of acute myeloid leukaemia following myelodysplastic syndrome after azacitidine treatment failure. Br J Haematol 2012;157:764–6.
45. Trowbridge JJ, Snow JW, Kim J, Orkin SH. DNA methyltransferase 1 is essential for and uniquely regulates hematopoietic stem and progenitor cells. Cell Stem Cell 2009;5:442–9.
46. Bröske A-M, Vockentanz L, Kharazi S, Huska MR, Mancini E, Scheller M, et al. DNA methylation protects hematopoietic stem cell multipotency from myeloerythroid restriction. Nat Genet 2009;41:1207–15.
47. Giachelia M, D'Alò F, Fabiani E, Saulnier N, Di Ruscio A, Guidi F, et al. Gene expression profiling of myelodysplastic CD34+ hematopoietic stem cells treated *in vitro* with decitabine. Leuk Res 2011;35:465–71.
48. Negrotto S, Ng KP, Jankowska AM, Bodo J, Gopalan B, Guinta K, et al. CpG methylation patterns and decitabine treatment response in acute myeloid leukemia cells and normal hematopoietic precursors. Leukemia 2012;26:244–54.
49. Ng KP, Ebrahem Q, Negrotto S, Mahfouz RZ, Link KA, Hu Z, et al. P53 Independent epigenetic-differentiation treatment in xenotransplant models of acute myeloid leukemia. Leukemia 2011;25:1739–50.
50. Miller KB, Kyungmann K, Morrison FS, Winter JN, Bennett JM, Neiman RS, et al. The evaluation of low-dose cytarabine in the treatment of myelodysplastic syndromes: a phase-III intergroup study. Ann Hematol 1992;65:162–8.